

# Design and optimization of BCCD in CMOS technology\*

GAO Jing (高静)<sup>1</sup>, LI Yi (李奕)<sup>1</sup>, GAO Zhi-yuan (高志远)<sup>1</sup>, and LUO Tao (罗韬)<sup>2\*\*</sup>

1. School of Electronic Information Engineering, Tianjin University, Tianjin 300072, China

2. Tianjin Key Laboratory of Cognitive Computing and Application, School of Computer Science and Technology, Tianjin University, Tianjin 300072, China

(Received 22 May 2016; Revised 20 June 2016)

©Tianjin University of Technology and Springer-Verlag Berlin Heidelberg 2016

This paper optimizes the buried channel charge-coupled device (BCCD) structure fabricated by complementary metal oxide semiconductor (CMOS) technology. The optimized BCCD has advantages of low noise, high integration and high image quality. The charge transfer process shows that interface traps, weak fringing fields and potential well between adjacent gates all cause the decrease of charge transfer efficiency (*CTE*). *CTE* and well capacity are simulated with different operating voltages and gap sizes. *CTE* can achieve 99.999% and the well capacity reaches up to 25 000 electrons for the gap size of 130 nm and the maximum operating voltage of 3 V.

**Document code:** A **Article ID:** 1673-1905(2016)05-0321-4

**DOI** 10.1007/s11801-016-6124-0

Nowadays, there are two main types of image sensors which are charge-coupled device (CCD) and complementary metal oxide semiconductor (CMOS)<sup>[1]</sup>. CCDs have attractive features of high sensitivity, low noise and high image quality, but they need high power consumption, high cost and complex process due to overlapping gates. On the other hand, CMOS image sensors with standard CMOS processes have advantages of high speed, low power consumption and low cost. However, CMOS image sensors have lower dynamic range and lower image quality compared with CCD. Fabricating CCD in CMOS technology is useful based on the advantages of low noise, high speed and high image quality. Adjacent non-overlapping single gates are separated by a narrow gap, and the maximum operating voltage is 3.3 V in CCD structure implemented in CMOS technology<sup>[2,3]</sup>. With device feature size shrinking, the gap size is narrowed continually and the performance of CCD fabricated in CMOS technology is comparable with conventional CMOS pixels<sup>[4,5]</sup>. The buried channel charge-coupled device (BCCD) structure implemented in CMOS technology was reported in Refs.[6]—[8], and the surface channel charge-coupled device (SCCD) in CMOS technology was reported in Refs.[9] and [10]. The BCCD structure has high charge transfer efficiency (*CTE*) of 99.9% and well capacity of 3 550 electrons<sup>[6,7]</sup>. *CTE* reached 99.99% with 3.3 V operation voltage, and well capacity achieved a few  $\text{Ke}^-/\mu\text{m}^2$  in Ref.[8]. The effects of fixed charge were alleviated by using a large negative voltage, and charge transfer inefficiency (*CTI*) ranged from  $5.7 \times 10^{-4}$  to  $7 \times 10^{-3}$  in Ref.[9]. *CTI* was reduced by

passivating the channel stop with p-well implanting in Ref.[10]. The CCD structure achieves high *CTE* and low noise charge accumulation so that it can be applied to X-ray imagers, time delay integration (TDI) image sensors, low-light-level image sensors and so on<sup>[6-10]</sup>.

The paper presents a BCCD structure in CMOS technology. Effects of gap size, the number of stored charge and the operating voltage on *CTE* are analyzed. The simulation results demonstrate that smaller size of gap and larger potential difference between adjacent gates can help charge transfer completely. In our design, device structure size, doping concentration and operating condition are optimized for getting the higher *CTE* and the larger well capacity.

Fig.1 shows the three dimension (3D) structure of BCCD array. It can be seen from Fig.1 that the array consists of single polysilicon gates, channels and channel stops<sup>[11]</sup>. We replace overlapping gates with single polysilicon gates separated by narrow gaps, and use p-type channel stops to isolate n-type buried channels. The p-type substrate has the thickness of 3  $\mu\text{m}$  and the concentration of  $1 \times 10^{15} \text{ cm}^{-3}$ . The n-type buried channel is formed by implanting phosphorus, and it has a peak concentration at 60 nm under the surface. Gate oxide is formed by depositing 8-nm-thick  $\text{SiO}_2$ . The thickness and width of p<sup>+</sup> doped polysilicon gates are 150 nm and 1  $\mu\text{m}$ , respectively. The width of gap between adjacent gates is 130 nm. We design BCCD structure with the help of technology computer aided design (TCAD). Fig.2 shows the cross sectional view of doping concentration diagram from the simulation structure of BCCD.

\* This work has been supported by the National Natural Science Foundation of China (Nos.61306070, 61404090 and 61674115).

\*\* E-mail: luo\_tao@tju.edu.cn

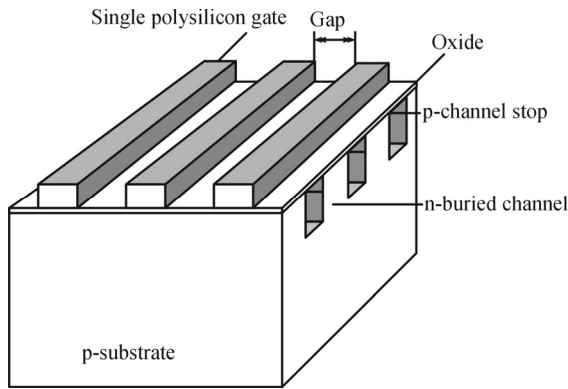


**Fig.1 Schematic diagram of 3D structure of BCCD array**

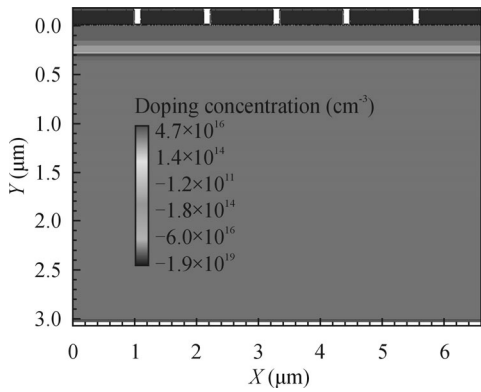


**Fig.2 Cross sectional view of doping concentration diagram from the simulation structure of BCCD**

Fig.3 shows the electrostatic potential profile in the bulk. The maximum potential well appears in the bulk, and charges are stored under the surface. The electrostatic potential is determined by gate voltage and the number of charge stored in the potential well. The electrostatic potential increases with raising the gate voltage and decreases with growing the number of charge stored in the potential well.

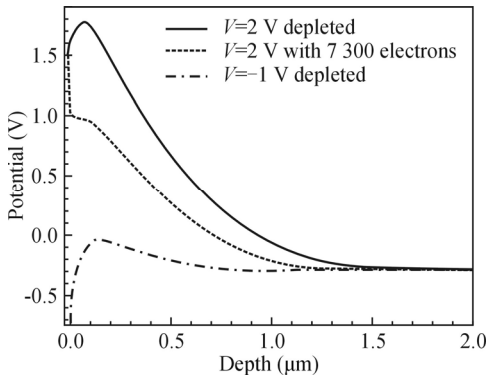
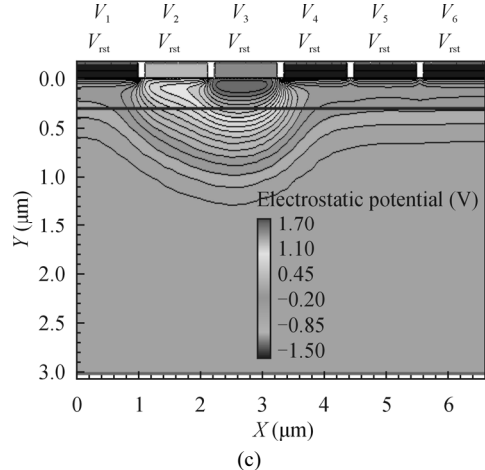
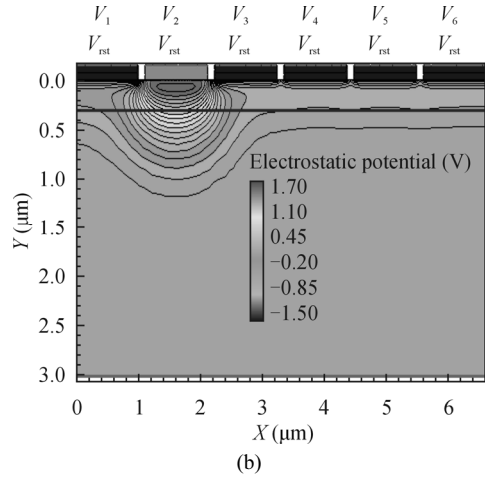
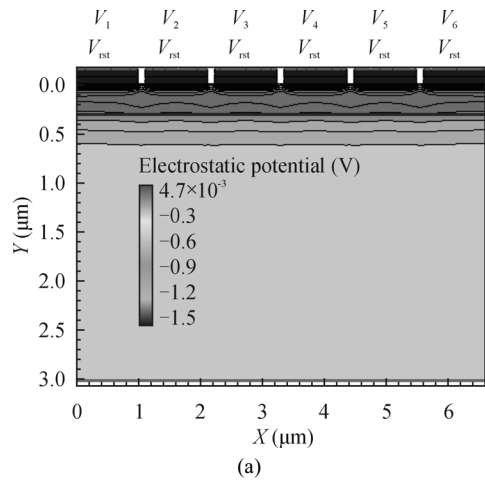


**Fig.3 Electrostatic potential profile below one gate with gate voltage of -1 V, 2 V depleted or 2 V with 7 300 electrons stored in potential well**

In the initial state of working process, all electrodes

are set to be  $V_{rst}$ . The buried channel is depleted completely, and the electrostatic potential distribution diagram is shown in Fig.4(a). And then  $V_{max}$  is applied to  $V_2$ , which creates a potential well. Photogenerated charges are stored in the potential well as shown in Fig.4(b). Next,  $V_2$  is set to be  $V_{max}/2$ , and  $V_3$  is set to be  $V_{max}$ . Potential difference is formed between  $V_2$  and  $V_3$ , which drives the charges from  $V_2$  to  $V_3$  as shown in Fig.4(c). Finally,  $V_2$  is driven back to  $V_{rst}$  and  $V_3$  remains  $V_{max}$  as shown in Fig.4(d). The charges are transferred from  $V_2$  to  $V_3$  fully. All of the charge transfers are completed according to the above sequence.



(c)

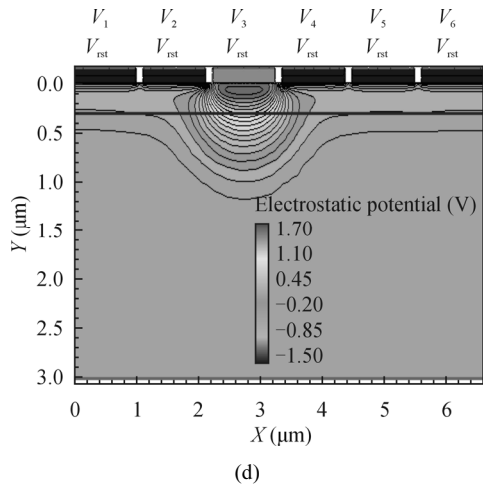


**Fig.4 Electrostatic potential distribution diagrams during charge transfer: (a) All electrodes are set to be  $V_{rst}$  and the buried channel is depleted completely; (b) Charges are stored in potential well created by  $V_2$ ; (c) Charges under  $V_2$  are transferred to  $V_3$ ; (d) Charges are transferred from  $V_2$  to  $V_3$  fully**

Charges are stored in the potential well in form of charge packet. Charge packets are transferred by three mechanisms which are thermal diffusion, self-induced drift and fringing field drift. Self-induced drift field is caused by charge gradient distribution. Charges in the same type repel each other and then redistributes. When the number of stored charge is small, transfer process is determined by thermal diffusion. The driving force provided by thermal diffusion is small which can lead to less *CTE*. Fringing field produced by the gate voltage is impacted by impurity doping concentration, the gap size and the different voltage between adjacent gates. Increasing gap size between adjacent gates is capable of weakening fringing field and enlarging potential pocket to stop charge transfer. Decreasing operating voltage also reduce fringing field and charge handling capability. Therefore, increasing operating voltage and shrinking gap size both have an effect on improving charge handling capability and *CTE*. In addition, the presence of interface traps is also the main factor of charge transfer failure. We use BCCD structure to transfer charge under surface which can avoid interface traps effectively.

*CTE* is the most important performance factor for evaluating the characterization of CCD. *CTE* between adjacent gates can be expressed as

$$CTE = \left( \frac{Q_N}{Q_0} \right)^{\frac{1}{n}}, \tag{1}$$

where  $n$  is the transfer times,  $Q_0$  is the number of stored charge, and  $Q_N$  is the number of transferred charge. In addition, charge handling capability is also an important factor in CCD structure which is decided by maximum well capacity. The higher gate voltage creates deeper potential well where more charges can be stored.

We evaluate *CTE* and charge handling capability with different gap sizes, different operating voltages and different numbers of stored electrons. Fig.5 shows the estimated *CTE* as a function of the number of stored electrons for gap sizes of 130 nm, 180 nm and 250 nm. It is obtained with  $V_{max}=3$  V and  $V_{rst}=-1$  V. From Fig.5 we can see that *CTE* is higher with smaller gap size. *CTE* reaches 99.999% when the gap size is 130 nm. With the increase of the number of stored electrons, *CTE* has an increasing trend for less than 10 000 stored electrons, and has a downward trend for more than 10 000 stored electrons. Weak self-induced drift field and potential pocket between adjacent gates are the main factors affecting *CTE* for less number of stored charges. With increasing the number of stored charge, the charge packet is closer to the Si/SiO<sub>2</sub> interface and is easier to be captured by interface traps. The presence of interface traps is the main factor affecting *CTE* for a large number of stored charges. Fig.6 shows simulated well capacity versus different maximum operating voltages. The well capacity is enhanced with higher maximum operating voltage. It reaches 25 000 electrons when maximum operating voltage  $V_{max}$  is 3 V and the width of gate is 0.5 μm. Fig.7 describes the estimated *CTE* as a function of the number of stored electrons with gap size of 130 nm for maximum operating voltage varying between 1.5 V and 3 V. Different operating voltages corresponds to different well capacities. The higher the maximum operating voltage, the greater the *CTE*.

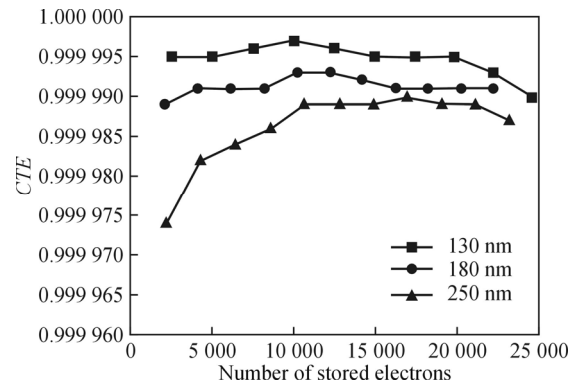


**Fig.5 *CTE* as a function of the number of stored electrons for different gap sizes**

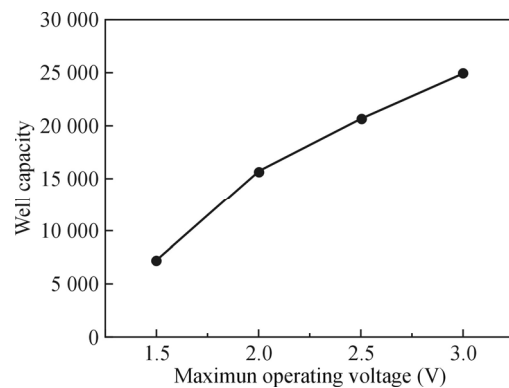


**Fig.6 Well capacity as a function of different operating voltages**

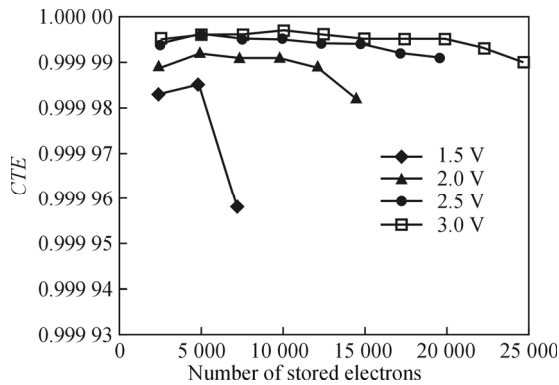


**Fig.7 CTE as a function of stored electrons for different operating voltages**

Detailed design and operation about the structure of BCCD fabricated by CMOS technology are presented. The analysis of charge transfer describes that weak fringing fields, potential pocket between adjacent gates and interface traps all lead to charge transfer failure. The simulation results demonstrate that CTE can be enhanced by narrowing the gap size and increasing the maximum operating voltage. The BCCD structure has CTE of 99.999% and well capacity of 25 000 electrons for gap size of 130 nm and maximum operating voltage of 3 V.

**References**

[1] Sanket Mehta, Arpita Patel, Jagrat Mehta, CCD or CMOS Image Sensor For Photography, IEEE Communications and Signal Processing, 0291 (2015).  
 [2] T. Yamada, Y. Kawakami, T. Nakano and N. Mutoh,

IEEE Transactions on Electron Devices **44**, 1580 (1997).  
 [3] O. Marcelot, M. Estribeau, V. Goiffon and P. Martin-Gonthier, IEEE Transactions on Electron Devices **61**, 844 (2014).  
 [4] Keith Fife, Abbas El Gamal, H.-S. Philip Wong, IEEE Journal of Solid-State Circuits **43**, 2990 (2008).  
 [5] F. Mayer, S. Pesenti, F. Barbier, H. Bugnet, J. Endicott, F. Devriere and T. Ligozat, CMOS Charge Transfer TDI With Front Side Enhanced Quantum Efficiency, International Image Sensor Workshop, (2015).  
 [6] Keith Fife, Abbas El Gamal and H.-S. Philip Wong, A 0.5 μm Pixel Frame-Transfer CCD Image Sensor in 110nm CMOS, IEEE International Electron Devices Meeting, 1003 (2007).  
 [7] Keith Fife, Abbas El Gamal and H.-S. Philip Wong, Design and Characterization of Submicron CCDs in CMOS, International Image Sensor Workshop, (2009).  
 [8] Alper Ercan, Luc Haspeslagh, Koen De Munck, Kiki Minoglou, Anne Lauwers and Piet De Moor, Prototype TDI Sensors in Embedded CCD in CMOS Technology, International Image Sensor Workshop, (2013).  
 [9] J. Borg and J. Johansson, IEEE Transactions on Electron Devices **58**, 2660 (2011).  
 [10] Olivier Marcelot, Romain Molina, Matthieu Bouhier and Pierre Magnan, IEEE Transactions on Electron Devices **63**, 1099 (2016).  
 [11] Piet De Moor, Jo Robbelein, Luc Haspeslagh, Pierre Boulenc, Alper Ercan, Kyriaki Minoglou, Anne Lauwers, Koen De Munck and Maarten Rosmeulen, Enhanced Time Delay Integration Imaging Using Embedded CCD in CMOS Technology, IEEE International Electron Devices Meeting, 461 (2014).